

Dynamic-Scaling Theory of Critical Ultrasonic Attenuation in Binary Liquids¹

R. A. Ferrell²

The critical slowing down that sets in near the critical point of a second-order phase transition is manifested in fluids by a diverging relaxation time for the long-wavelength order-parameter fluctuations. This divergence has a profound effect on all of the transport properties. In sound propagation, the adiabatic compressions and dilations produce temperature swings which the order-parameter fluctuations can follow fully only if the sound frequency is smaller than the relaxation rates in the fluid. As the critical point is approached this condition is violated and a lagging, or hysteretic, response results. As demonstrated by Clerke *et al.*, the known amplitude of the temperature swings leads to a prediction of ultrasonic attenuation at the critical point that agrees, in magnitude, exactly with that found by Harada *et al.* The theoretically predicted scaling function that describes how the attenuation and dispersion vary as the critical point is approached is in good agreement with the experimental findings of Garland and Sanchez.

KEY WORDS: critical phenomena; dynamic scaling; liquid mixtures; ultrasonic attenuation.

1. INTRODUCTION

In this brief review of the critical ultrasonic attenuation near the consolute point of a binary liquid, it is well to emphasize that the attenuation is simply one aspect of the general phenomena of sound propagation, as described, in general, by a complex velocity. The attenuation at some frequency $\omega > 0$ is associated with the imaginary part of the velocity, while the real part of the velocity determines the dispersive sonic behavior of the fluid. For the sake of brevity, I do not discuss here the critical dispersion

¹ Paper presented at the Tenth Symposium on Thermophysical Properties, June 20–23, 1988, Gaithersburg, Maryland, U.S.A.

² Center for Theoretical Physics, Department of Physics and Astronomy, University of Maryland, College Park Maryland, 20742, U.S.A.

(the interested reader is referred to our more detailed paper [1]), but it will become clear that a complete theory is obliged to deal with both attenuation and dispersion as two parts of the same problem. A fortiori, the theoretical expression for the velocity must reduce in the limit of vanishing frequency ($\omega \rightarrow 0$ and $\lambda \rightarrow \infty$, the long-wavelength limit) to the formula that follows from straightforward thermodynamics. Thus, thermodynamics provides a kind of “ $\omega = 0$ boundary condition,” or check, on the theory.

In the neighborhood of the critical point, thermodynamics gives the following expression for the velocity of sound propagation, u :

$$u^{-2} = u_c^{-2} - \frac{g^2}{T_c C_p} \quad (1)$$

where C_p is the specific heat per unit mass at constant pressure, T_c is the critical temperature, u_c is the sound velocity at T_c , and

$$g = \frac{T_c S'_c}{V_c} \quad (2)$$

is a kind of dimensionless “coupling constant.” The critical volume per unit mass is denoted by V_c , while S'_c is the derivative of the entropy with respect to the pressure parallel to the λ line of critical points, i.e., $S'_c = (\partial S / \partial P)_{\Delta T}$. The distance away from the λ line, as measured on the temperature scale, is $\Delta T = T - T_c(P)$. For a binary liquid, the second term of Eq. (1) is generally small compared to the first, which permits the linearization

$$u = u_c + \frac{g_2 u_c^3}{2 T_c C_p} \quad (3)$$

This linear variation of the sound velocity with C_p^{-1} is illustrated by the “Barmatz–Rudnick plot,” shown as the solid line in Fig. 1, and is familiar from measurements by Barmatz and Rudnick [2] in the neighborhood of the λ transition in liquid ^4He . The λ transition and the phase transition at the consolute point of a binary liquid are similar in that the pressure signal is not coupled directly to the order parameter. As a consequence, the Barmatz–Rudnick formula for ^4He is equivalent to Eq. (3).

In 1816, Laplace [3] showed that Newton had made an error in calculating the velocity of sound in gases. By recognizing that the sound velocity has to be calculated from the adiabatic, rather than from the isothermal, compressibility, Laplace [3] accounted for the 20% discrepancy between Newton’s computation and the experimental data. This “entropy-clamping” condition also plays an essential role in liquids. In par-

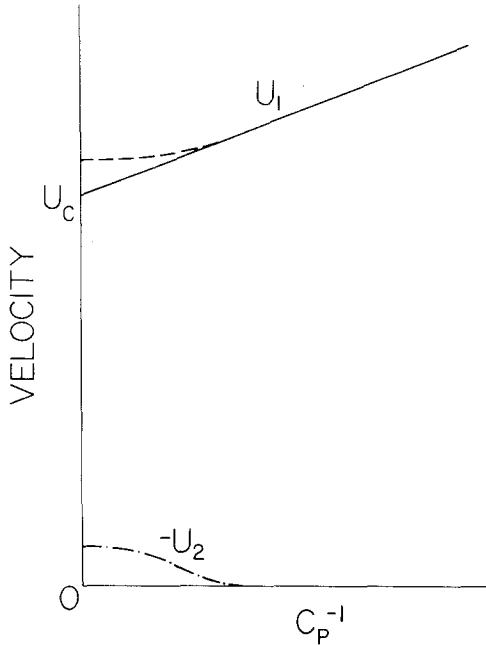


Fig. 1. Barmatz–Rudnick plot for the sound velocity versus reciprocal of the thermodynamic specific heat, both in arbitrary units. At the consolute point the velocity is u_c . For a nonvanishing frequency the real part, u_1 , deviates from its thermodynamic value (dashed curve) and the imaginary part, u_2 , develops a nonvanishing negative value that results in sound absorption.

ticular, it implies that the pressure swings are necessarily accompanied by temperature swings, in order that the entropy should remain constant. The temperature swing obviously brings into play the thermodynamic response function relating entropy and temperature, namely, C_p . Rather than work with the variation of T , it is more convenient to use ΔT . Entropy clamping then yields

$$\left(\frac{\partial \Delta T}{\partial P}\right)_s = -\frac{(\partial S/\partial P)_{\Delta T}}{(\partial S/\partial \Delta T)_P} \approx -\frac{T_c S'_c}{C_p} = -g \frac{V_c}{C_p} \tag{4}$$

In the neighborhood of the critical point, the isentropic compressibility is

$$\beta_s = \beta_s^c + \frac{S'_c}{V_c} \left(\frac{\partial \Delta T}{\partial P}\right)_s \tag{5}$$

Combining Eqs. (4) and (5) yields Eq. (1). From the definition of the coupling constant in Eq. (2), as well as from Eq. (4), we see that g can be obtained from purely static measurements. In the binary system 3-methylpentane-nitroethane, g has been determined by Clerke et al. [4] to be -0.34 ± 0.01 .

2. ATTENUATION OF SOUND

At a finite frequency, $\omega \neq 0$, the linearized equation of motion relating the variation in ΔT to the variation in P depends on the isentropic derivative in Eq. (4), which continues to remain valid, even in this nonthermodynamic situation. But as the consolute point is approached, critical slowing down implies that the temperature variations will not remain in phase with the pressure swings. In other words, in Eq. (4), C_P becomes a complex, frequency-dependent linear response function. Thus, the sound velocity u becomes dispersive and, by analyticity, acquires an imaginary, dissipative part. The temperature dependence of the deviation of $u_1 = \text{Re}u$ and $-u_2 = -\text{Im}u$ from their thermodynamic values as functions of the thermodynamic quantity C_P^{-2} is illustrated schematically in Fig. 1 by the dashed and dot-dashed curves, respectively. We see that the theory of ultrasonic attenuation is intimately connected with that of the frequency-dependent specific heat. Before proceeding to develop this idea further, we note that this approach builds firmly on elementary thermodynamic principles, with no need for additional hypotheses. In particular, it is not necessary to postulate a bulk viscosity.

As the critical point is approached, the relaxation rate γ of the slowest ($\lambda = \infty$) fluctuation mode approaches zero as $(\Delta T)^{zv}$, where the exponent is $zv \simeq (3.05) \cdot (0.63) \simeq 1.9$. Thus, an ultrasonics experiment performed at a finite frequency, ω' , crosses over into a nonthermodynamic regime in which the slow modes, which do not have time to relax in one period of sound propagation, do not contribute to the specific heat. This is illustrated in Fig. 2. In the extreme nonthermodynamic regime, on the $\gamma = 0$ axis, the relevant variable for determining the strength of the linear entropy response, C_P , is not ΔT but the frequency ω . The effect on u of this deviation from the thermodynamic behavior is illustrated by the vertical intercepts of the dashed and dot-dashed curves in Fig. 1. To obtain this frequency-dependent response function right at the critical point, we linearize the specific heat relative to its large noncritical background,

$$C_P^{-1} \equiv (B + C)^{-1} \simeq B^{-1} - B^{-2}C \quad (6)$$

and write $C(\Delta T, 0) \propto (\Delta T)^{-\alpha} \simeq (\Delta T)^{-0.11}$ as

$$C(\Delta T, 0) \propto \gamma^{-0.06} \quad (7)$$

Crossing over into the nonthermodynamic regime, we replace γ by $-i\omega/a$ and obtain

$$C(0, \omega) \propto \left(\frac{-i\omega}{a} \right)^{-0.06}$$

where a , a numerical parameter of the order of magnitude of unity, is the slope of the dashed line in Fig. 2. The replacement of the temperature-dependent rate by the frequency expresses the principle of dynamic scaling. This feature and the occurrence of the factor of $-i$, as required by the relaxational nature of the concentration fluctuations, are exhibited explicitly, and quite naturally, by the detailed theory [1]. It follows that the critical portion α_c of the attenuation per wavelength λ at the critical point (consolute point) is given (neglecting the noncritical background) by

$$\lambda\alpha_c = \frac{2\pi u_1}{\omega} \alpha_c \simeq \frac{2\pi u_c}{\omega} \alpha_c \propto \text{Im } C(0, \omega) \propto \omega^{-0.06} \quad (8)$$

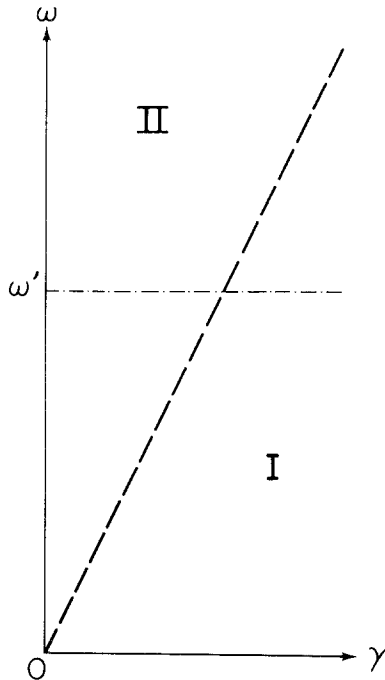


Fig. 2. Frequency and rate plane illustrating the working of dynamic scaling. Both ω and γ are in arbitrary units. Crossover occurs from quasi-thermodynamic to nonthermodynamic behavior at the dashed line $\omega = a\gamma$. As the critical point is approached at a constant finite frequency ω' , as shown by the dot-dashed line, γ dependence changes to ω dependence.

A cautionary note is in order at this point. The linearization in Eq. (6) depends upon the inequality $C \ll B$. This may not be satisfied for all binary liquids and is certainly not satisfied in the case of liquid helium. In such cases C has to be kept in the denominator of C_p^{-1} , with the consequence that $\text{Im } C_p^{-1}$ depends upon $\text{Re } C$ as well as upon $\text{Im } C$. For the liquid helium λ transition, $\alpha \simeq 0$, so that in the vicinity of the λ point $\text{Re } C$ is logarithmically dependent upon the magnitudes of ω and γ , and not simply on their ratio, the reduced frequency $\Omega = \omega/\gamma$. This leads to a lack of scaling at the critical point, unless the data are appropriately processed, an unusual feature fully confirmed by experiment.

To exhibit experimental data for a binary fluid at its consolute point it is convenient to divide α_c by ω^2 , in order to isolate the noncritical background. In Fig. 3, the critical point attenuation data of Harada and co-workers [5] is plotted in this way versus $\omega^{-1.06}$. The straight-line behavior, with the predicted value for the slope, confirms the above theory, whose only inputs are general thermodynamic relations and dynamic scaling. The fact that the magnitude of the attenuation is accurately accounted for, with no adjustable parameters, indicates that the adiabatic temperature swings are the correct physical mechanism for the critical attenuation.

3. DYNAMIC SCALING ATTENUATION

The determination of the full course of the attenuation as a function of temperature, at a given frequency, is a more complicated problem, which

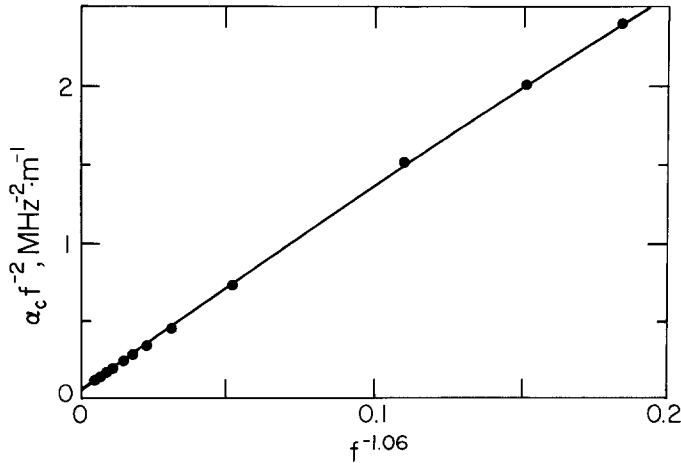


Fig. 3. $\alpha_c/f^{-1.06}$, where α_c is the critical-point attenuation, and $f = \omega/2\pi$ is the frequency in MHz. The linear fit confirms the theory and the intercept determines the background attenuation.

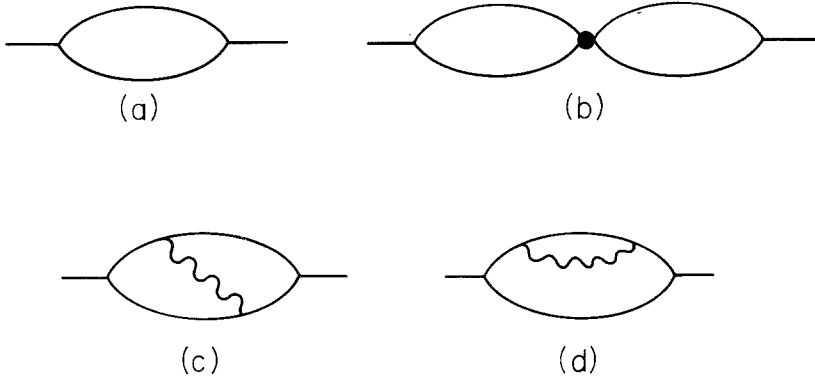


Fig. 4. Specific-heat graphs to two-loop order. The wavy lines in c and d correspond to the hydrodynamic shear modes.

we have attacked [1] using perturbation theory; the relevant Feynman graphs are shown in Fig. 4. The calculation is complicated by the necessity of accounting for a variety of static and dynamic interactions. The lowest-order static correction to the single-loop graph in Fig. 4a is Fig. 4b, which takes into account the four-point interaction and is an essential ingredient for obtaining the correct thermodynamic exponent. Figures 4c and d represent the coupling to the shear modes. While Fig. 4d corresponds to the familiar correction to the order-parameter relaxation rate, the exchange graph, Fig. 4c, is unique to the specific heat and is needed for establishing the correct value for the parameter a . This, in turn, determines the temperature at which the attenuation falls to one-half of its critical point value.

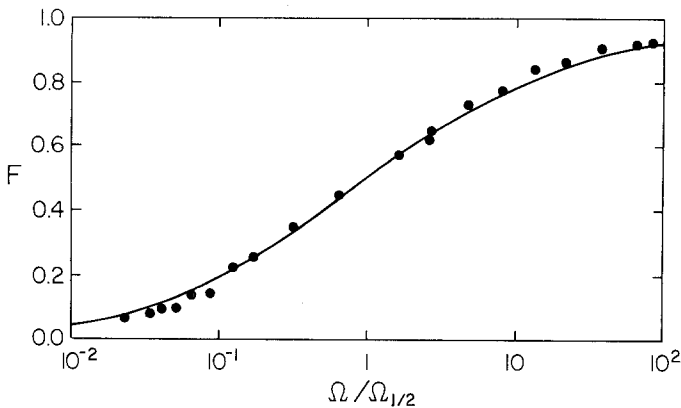


Fig. 5. Normalized attenuation function $F \equiv F(\Omega)$ vs $\Omega/\Omega_{1/2}$. $\Omega_{1/2}$ is the value of the dimensionless frequency Ω for which $F(\Omega) = \frac{1}{2}$.

From a more general theoretical point of view, omission of such graphs is known to violate gauge invariance in quantum electrodynamics. The "attenuation function," $F(\Omega)$, defined as the attenuation divided by its value at the critical point, for the same frequency, is exhibited in Fig. 5. When $\Omega \rightarrow \infty$, $F(\Omega) \rightarrow 1$ asymptotically, while for $\Omega \ll 1$, $F(\Omega) \propto \Omega$. In plotting Fig. 5 we used the following approximate formula, which we found [1] to capture the essential features of this function:

$$F(\Omega) = [1 + 0.414(\Omega/\Omega_{1/2})^{-1/2}]^{-2} \quad (9)$$

The scale parameter $\Omega_{1/2}$ corresponds to the halfway temperature referred to above. It is seen that the agreement with the data of Garland and Sanchez [6], at 3 MHz is quite satisfactory. The observed frequency scale is similarly in good agreement with the theoretical estimate of $\Omega_{1/2} \simeq 2$.

4. COEXISTENCE CURVE

All the above discussion has related to a binary liquid mixed at exactly the critical concentration. Upon cooling in the single-phase regime, such a fluid will arrive at the consolute point and a separation into two coexistence phases will start to take place. The approach to the second-order phase transition is characterized by the diverging correlation length,

$$\xi \propto (\Delta T)^{-\nu} \quad (10)$$

where $\nu = 0.63$. The diverging relaxation time, responsible for the critical ultrasonic attenuation, whose temperature dependence we have written above as

$$\gamma^{-1} \propto (\Delta T)^{-z\nu} \quad (11)$$

can equally well be expressed in terms of the correlation length as

$$\gamma^{-1} \propto \xi^z \quad (12)$$

with $z \simeq 3.05$. If the concentration deviates by some amount s from its critical value, then Eq. (11) no longer applies and Eq. (12) must instead be used. In this case, ξ increases as the temperature is lowered, but it does not diverge. When the coexistence line is reached and a first-order transition takes place, ξ has the finite limiting value

$$\xi_{\text{coex}} \propto |s|^{-\nu/\beta} \quad (13)$$

where $\beta \simeq 0.325$ is the order-parameter critical exponent. As a result, the

relaxation rate does not drop to zero, as it does at the consolute point but, instead, takes on the nonvanishing limiting value

$$\gamma_{\text{coex}} \propto |s|^{z\nu/\beta} \tag{14}$$

It follows that, on the coexistence curve away from the consolute point, the frequency dependence of the critical portion of the ultrasonic attenuation is given by

$$\frac{\alpha_c}{\omega} \propto \omega^{-1.06} F(\Omega_{\text{coex}}) = \gamma_{\text{coex}}^{-1.06} X F(\Omega_{\text{coex}}) \propto X F(\Omega_{\text{coex}}) \tag{15}$$

where

$$X \equiv (c\Omega_{\text{coex}})^{-1.06} \tag{16}$$

and

$$\Omega_{\text{coex}} \equiv \frac{\omega}{\gamma_{\text{coex}}} \tag{17}$$

The numerical factor is

$$c = \frac{3 + 2\sqrt{2}}{\Omega_{1/2}} \approx 2.9 \tag{18}$$

The final form of the right-hand side of Eq. (15) is plotted versus X as the solid curve in Fig. 6. For comparison, the dashed straight line shows the

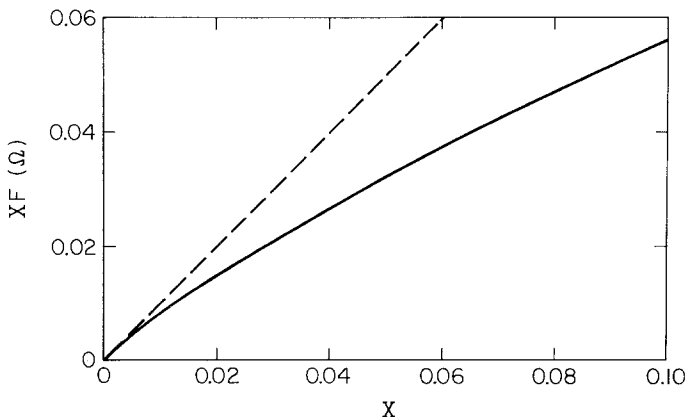


Fig. 6. Frequency dependence of α_f/ω^2 as a function of $X \propto \Omega^{-1.06}$, with $\Omega \equiv \Omega_{\text{coex}} = \omega/\gamma_{\text{coex}}$, where γ_{coex} is the relaxation rate on the coexistence curve. The dashed straight line shows the consolute point behavior in Fig. 3, while the curve illustrates the reduction in attenuation for a noncritical concentration.

linear relationship that has already been exhibited in Fig. 3 for the consolute point. The downward curvature and the reduction below the dashed straight line are a consequence of the factor $F(\Omega_{\text{coex}})$ in Eq. (15), with the smaller values for Ω_{coex} and $F(\Omega_{\text{coex}})$ occurring for the larger values of X .

5. SUMMARY

In summarizing this brief review I would like again to call attention to the excellent agreement between $g = -0.34 \pm 0.01$, the direct thermodynamic determination of the coupling constant by Clerke and Sengers, as reported by Clerke et al. [4], and its indirect measurement, $|g| = 0.33 \pm 0.03$, by means of the attenuation data of Harada et al. [5]. It is worth emphasizing that this agreement leaves little room for doubting that the physical mechanism for the attenuation is the temperature oscillations resulting from the adiabatic compressions and rarefactions. The frequency dependence of the attenuation per wavelength, with the exponent $\alpha/zv \simeq \alpha/1.9 \simeq 0.06$, is further confirmation of the essential role of the specific heat. Finally, the predictions of the theory for the frequency scale parameter $\Omega_{1/2}$ and for the shape of the scaling function $F(\Omega)$ are in encouragingly good accord with the experimental findings of Garland and Sanchez [6]. It is likely, however, that the last word has not been said regarding these more detailed aspects of the theory.

ACKNOWLEDGMENTS

It is a pleasure to acknowledge the assistance of B. Mirhashem in preparing the manuscript and the support of the National Science Foundation under Grants DMR-79-001172, DMR-82-05356, and DMR-85-06009.

REFERENCES

1. R. A. Ferrell and J. K. Bhattacharjee, *Phys. Rev.* **A31**:1788 (1985).
2. M. Barmatz and I. Rudnick, *Phys. Rev.* **170**:224 (1968).
3. P. S. Laplace, *Ann. Chim. Phys.* **iii**:238 (1816).
4. E. A. Clerke, J. V. Sengers, R. A. Ferrell, and J. K. Bhattacharjee, *Phys. Rev.* **A27**:2140 (1983).
5. Y. Harada, Y. Suzuki, and Y. Ishida, *J. Phys. Soc. Jpn.* **48**:703 (1980); see also Y. Ishida and Y. Harada, *Jpn. J. Appl. Phys.* **19**:1563 (1980).
6. C. W. Garland and G. Sanchez, *J. Chem. Phys.* **79**:3090 (1983); see also G. Sanchez and C. W. Garland, *J. Chem. Phys.* **79**:3100 (1983).